Available online at www.sciencedirect.com
ScienceDirect
Tunnelling and Underground Space Technology 22 (2007) 185–205
Tunnelling and Underground Space Technology
incorporating Trenchless Technology Research
www.elsevier.com/locate/tust

A numerical approach to the hyperstatic reaction method for the dimensioning of tunnel supports

P.P. Oreste *

Dept. of Ingegneria del territorio, dell'ambiente e delle geotecnologie (DITAG), Politecnico di Torino, Italy

Received 28 April 2005; received in revised form 24 April 2006; accepted 13 May 2006
Available online 10 August 2006

Abstract

The hyperstatic reaction method is particularly suitable for the dimensioning of support structures. This method simulates the interaction between the support and rock surrounding the tunnel through independent "Winkler" type springs. It requires the definition of the active loads that are applied directly to the support structure by the rock mass. Further passive loads are due to the reaction of the rock mass to the displacement of the support structure.

A numerical approach to the hyperstatic reaction method is presented in this paper. The parameters that condition the calculation and the dimensioning techniques of the support structures, on the basis of the results of the method, are also presented. A specific code, named FEMSUP, was developed using a FEM framework, to perform calculations with the HRM. This code is able to consider the effective geometry of the support and the horizontal active loads that are different from the vertical ones; it is therefore able to analyse the rock mass–structure interaction in detail.

An extensive parametric analysis performed using FEMSUP has made it possible to define the necessary support structures (steel sets incorporated into a shotcrete lining) in a wide number of cases that cover the conditions that are generally encountered in excavation practice. Ten design tables were drawn up to summarise the results of the parametric analyses. From an examination of the tables, it is possible to verify the influence of the various calculation parameters on the dimensioning of the support structure and to obtain rough indications on the entity of the support structures in the preliminary stages of a project.

1. Introduction

Numerical methods that discretisize the entire medium around a tunnel are not commonly used for the dimensioning of support structures due to the needed computational efforts. These structures are usually simulated through beam elements that are connected to the nodes of a numerical model, with the consequences that the displacements of the structure are closely linked to the deformations of the rock mass around the tunnel. If a correct interface, which does not permit the development of normal tensile stresses, is not placed between the support and the tunnel perimeter, bending moment results are different from the true ones, both from the qualitative and quantitative point of view. Furthermore, the times necessary to prepare the models, carry out the calculations and interpret the results are usually very long.

Simplified analytical methods, such as the convergence-confinement method (Rechsteiner and Lombardi, 1974; Hoek and Brown, 1980; Brown et al., 1983; Panet, 1995; Oreste, 2003), are able to stimulate the mean displacements of the support structure and the mean loads acting on it, but they do not supply the bending moments or the shear forces that are necessary, together with the normal forces, for its correct dimensioning. The relative stiffness solution (Einstein and Schwartz, 1979) is a very interesting and simplified approach which allows one to obtain, for circular tunnels and elastic ground, the bending moments and axial forces in the support structure. This method, however, considers the support realised in the tunnel without any

* Tel.: +39 0 11 5647608; fax: +39 0 11 5647699.
E-mail address: piorest@tin.it.

0886-7798/$ - see front matter © 2006 Elsevier Ltd. All rights reserved.
doi:10.1016/j.tust.2006.05.002

previous convergence (relaxation) of the rock mass surrounding the tunnel.

The hyperstatic reaction method (Duddeck and Erdmann, 1985; Bouvard-Lecoanet et al., 1988; Leca and Clough, 1992) (Fig. 1), which belongs to the numerical method category, is instead particularly suitable for the dimensioning of support structures. This method simulates the interaction between the support and rock surrounding the tunnel through many independent "Winkler" type springs: the reason it is named hyperstatic is due to the great number of connections of the support structure with the outside. The method requires definition of the active loads that are applied directly to the support structure by the rock mass; these active loads can be estimated from the technical literature (Barton et al., 1974; Barton, 2002; Unal, 1983; Goel et al., 1995, 1996; Singh et al., 1992, 1997; Bieniawski, 1989). They can also be estimated on the basis of the in situ monitoring, using back-analysis procedures. Further passive loads are due to the reaction of the rock mass to the displacement of the support structure.

The support–rock interaction influences the stress state in the structure to a great extent and this interaction depends on the mechanical characteristics of the rock mass. As these are only generally known with a certain approximation, it is often necessary to carry out parametric or probabilistic type analyses in order to be able to completely describe the uncertainty on the stress state of the support structure. These types of analyses need many calculations and the hyperstatic reaction method results to be particularly suitable for this purpose, due to the short time it requires.

Three parameters influence the stress state in a support structure more than the others when a calculation with the hyperstatic reaction method is made: the applied active loads, the stiffness of the structure (normal stiffness and bending stiffness) and the pressure-displacement relation that describes the interaction between the structure and the rock mass.

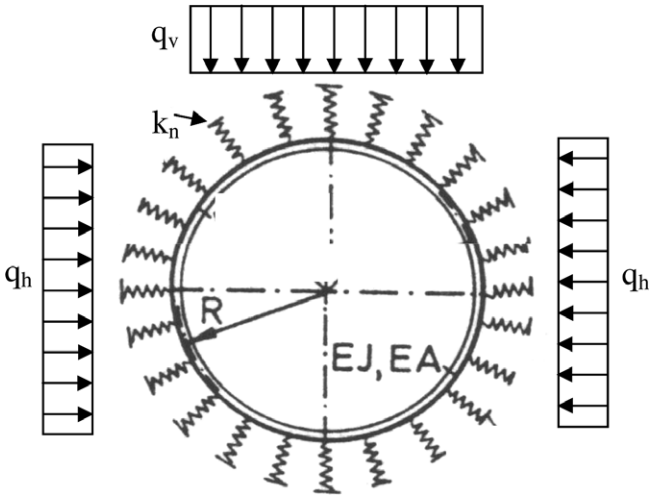

Fig. 1. Calculation scheme of support structures with the hyperstatic method. Active loads are applied to the tunnel support by the rock mass in the roof (vertical loads, q_v) and on the lateral sides (horizontal loads, q_h). The active loads are independent of the displacements that develop in the support and at the rock-support interface. Key: q_v: vertical load; q_h: horizontal load; k_n: stiffness of the interaction springs; R: tunnel radius; $E \cdot J$ and $E \cdot A$: bending and normal stiffness of the support.

The reaction produced by the rock mass on the deformations of the support is also a function of the stiffness of the structure. This only depends on the mechanical and geometrical characteristics of the support. Its dimensioning should therefore be carried out in a succession of approximations, working on variations of input data and verifying the compatibility of the stress and strain state with the maximum admissible conditions.

Steel sets incorporated into a shotcrete lining are one of the most commonly used preliminary support methods. Because of the bi-dimensional approach of the calculation method and the composite nature of the structure, it is necessary to determine the characteristics of an equivalent continuous support that must be introduced into the calculation. The interpretation of the results relative to the equivalent support is a decisive step for the dimensioning of the different individual structural components and it is a step that requires particular care.

A numerical approach to the hyperstatic reaction method is presented in this paper. The parameters that condition the calculation and the dimensioning techniques of the support structures, on the basis of the results of the method, are also presented.

A specific code, named FEMSUP, was developed using an FEM framework, to perform calculations with the hyperstatic reaction method (HRM). This code is able to consider the effective geometry of the support and horizontal active loads that are different from the vertical ones; it is therefore able to analyse the rock mass-structure interaction in detail.

The results of an extensive parametric analysis (4200 analyses) using this calculation code has made it possible to prepare 10 design tables for the preliminary evaluation of the type of support that is necessary, when the applied external loads and the geomechanical quality of the rock mass are known. Application examples on real cases show how the calculation code and the indications that can be obtained from the design tables, should be used.

2. The mathematical formulation of the method

The fundamental hypothesis on which the numerical approach to the hyperstatic reaction method is based, is that of subdividing the support structure into a finite number of linear sub-dominions, called elements (for which it is possible to describe the stress–strain law in a simple way), which are connected to the outside through stiffnesses distributed over the nodes. The support structure is therefore represented, in the calculation, by mono-dimensional elements that are able to develop bending moments, axial forces and shear forces (Fig. 2).

The beam element i is defined by the following parameters: the inertia modulus J and area A of the transversal

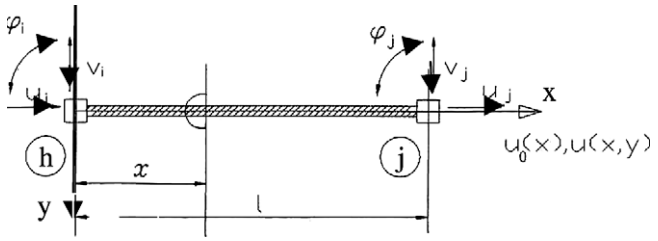

Fig. 2. Scheme of the behaviour of a beam-type finite element, with reference to the local Cartesian coordinates. Key: h: the initial node; j: the final node; u: the axial displacement; v: the transversal displacement; φ: the rotation; x and y: the local Cartesian coordinates.

section, the elastic modulus E of the constituent material and length L_i (distance between the terminal connecting nodes). In bi-dimensional methods, reference is made to a unitary thickness and therefore the parameters J and A should also be calculated considering the sum of the inertia modules and the areas that are involved in the support for a unitary length in the direction of the tunnel axis.

The unknown parameters of the problem are the displacement components of the nodes of the discretized structure. Once these unknown displacements are known, it is possible to obtain the stress characteristics on the inside of each element and therefore also along the entire length of the support structure.

The evaluation of the unknown displacements is made through the definition of the global stiffness matrix of the entire structure and of its connections to the surrounding environment. The global stiffness matrix is obtained starting from the local stiffness matrices of each single element, and then passing to their assembly.

The local stiffness matrix z_i of the i element is obtained by placing the work produced by the inner forces of the finite element equal to that produced by the external nodal forces, which are evaluated according to a local reference system (Huebner et al., 2001).

One therefore has:

$$z_i \cdot s_i = G_i + R_i \tag{1}$$

s_i: the vector of the displacements in nodes h and j of element i, evaluated according to the local reference system:

$$s_i = \lfloor\, u_{h,i} \quad u_{j,i} \quad v_{h,i} \quad \varphi_{h,i} \quad v_{j,i} \quad \varphi_{j,i} \,\rfloor$$

u and v: the axial and transversal displacement in the local reference system;

φ: the rotation of the element in correspondence to the nodes;

G_i and R_i: the external nodal forces and the nodal forces applied by the neighbouring elements, which are evaluated according to the local reference system;

$$G_i^T = \left[\boxed{G_{xh,i} \quad G_{yj,i}} \;\; \boxed{G_{yh,i} \quad G_{zh,i} \quad G_{yj,i} \quad G_{zj,i}}\right]^T = \left[G_{a,i}^T \quad G_{b,i}^T\right]$$
$$R_i^T = \left[\boxed{R_{xh,i} \quad R_{xj,i}} \;\; \boxed{R_{yh,i} \quad R_{zh,i} \quad R_{yj,i} \quad R_{zj,i}}\right]^T = \left[R_{a,i}^T \quad R_{b,i}^T\right]$$

G_i and R_i give the axial forces in the initial node h and in the final node j of the generic element i in the first two elements (Fig. 2), the transversal forces and the bending moment in the initial node h in the third and fourth elements, and the transversal force and the bending moment in the final node j in the fifth and sixth elements.

Eq. (1), re-written in explicit form, becomes:

$$\begin{bmatrix}
\frac{E\cdot A}{L_i} & -\frac{E\cdot A}{L_i} & 0 & 0 & 0 & 0 \\
-\frac{E\cdot A}{L_i} & \frac{E\cdot A}{L_i} & 0 & 0 & 0 & 0 \\
0 & 0 & \frac{12\cdot E\cdot J}{L_i^3} & \frac{6\cdot E\cdot J}{L_i^2} & -\frac{12\cdot E\cdot J}{L_i^3} & \frac{6\cdot E\cdot J}{L_i^2} \\
0 & 0 & \frac{6\cdot E\cdot J}{L_i^2} & \frac{4\cdot E\cdot J}{L_i} & -\frac{6\cdot E\cdot J}{L_i^2} & \frac{2\cdot E\cdot J}{L} \\
0 & 0 & -\frac{12\cdot E\cdot J}{L_i^3} & -\frac{6\cdot E\cdot J}{L_i^2} & \frac{12\cdot E\cdot J}{L_i^3} & -\frac{6\cdot E\cdot J}{L_i^2} \\
0 & 0 & \frac{6\cdot E\cdot J}{L_i^2} & \frac{2\cdot E\cdot J}{L_i} & -\frac{6\cdot J}{L_i^2} & \frac{4\cdot J}{L_i}
\end{bmatrix} \cdot \begin{bmatrix} u_{h,i} \\ u_{j,i} \\ v_{h,i} \\ \varphi_{h,i} \\ v_{j,i} \\ \varphi_{j,i} \end{bmatrix} = \begin{bmatrix} R_{xh,i}+G_{xh,i} \\ R_{xj,i}+G_{xj,i} \\ R_{yh,i}+G_{yh,i} \\ R_{zh,i}+G_{zh,i} \\ R_{yj,i}+G_{yj,i} \\ R_{zj,i}+G_{zj,i} \end{bmatrix}$$

z_i (2)

In the global Cartesian reference system, the nodal displacements q are connected to s through the following matrix expression:

$$s_i = \lambda_i \cdot q_{h\div j,i} \tag{3}$$

where

$$q_{h\div j,i} = \begin{bmatrix} w_{h,i} \\ z_{h,i} \\ \varphi_{h,i} \\ w_{j,i} \\ z_{j,i} \\ \varphi_{j,i} \end{bmatrix} = \begin{bmatrix} q_i \\ q_{i+1} \end{bmatrix} \quad \text{and}$$

$$\lambda_i = \begin{bmatrix}
\cos\alpha_i & \sin\alpha_i & 0 & 0 & 0 & 0 \\
0 & 0 & 0 & \cos\alpha_i & \sin\alpha_i & 0 \\
\sin\alpha_i & -\cos\alpha_i & 0 & 0 & 0 & 0 \\
0 & 0 & 1 & 0 & 0 & 0 \\
0 & 0 & 0 & \sin\alpha_i & -\cos\alpha_i & 0 \\
0 & 0 & 0 & 0 & 0 & 1
\end{bmatrix}$$

$q_{h\div j,i}$ is the vector of the nodal displacements of element i; q_i is the vector of the nodal displacement of node i; w and z are the displacements along axis x and along axis y of the global Cartesian reference system; α_i is the angle that forms the local Cartesian reference system of element i with respects to the global Cartesian reference system.

In the same way, in the global Cartesian reference system, the nodal forces are given by the following matrix expressions:

$$G_i = \lambda_i \cdot F_{h\div j,i} \tag{4}$$
$$R_i = \lambda_i \cdot Q_{h\div j,i} \tag{5}$$

where

$$F_{h\div j,i}=\begin{bmatrix}F_{xh,i}\\F_{yh,i}\\M_{h,i}\\F_{xj,i}\\F_{yj,i}\\M_{j,i}\end{bmatrix}=\begin{bmatrix}F_i\\F_{i+1}\end{bmatrix}\qquad Q_{h\div j,i}=\begin{bmatrix}Q_{xh,i}\\Q_{yh,i}\\Q_{Mh,i}\\Q_{xj,i}\\Q_{yj,i}\\Q_{Mj,i}\end{bmatrix}=\begin{bmatrix}Q_i\\-Q_{i+1}\end{bmatrix}$$

Making the necessary substitutions, it becomes possible to write in the global Cartesian reference system the following equation:

$$z_i\cdot\lambda_i\cdot q_{h\div j,i}=(G_i+R_i)=\lambda_i\cdot(F_{h\div j,i}+Q_{h\div j,i})$$

And therefore:

$$(\lambda_i^{\mathrm{T}}\cdot z_i\cdot\lambda_i)\cdot q_{h\div j,i}=F_{h\div j,i}+Q_{h\div j,i}$$

which can be re-written in the following form:

$$k_i\cdot q_{h\div j,i}=F_{h\div j,i}+Q_{h\div j,i}\tag{6}$$

where k_i is the local stiffness matrix of the element i in the global Cartesian reference system:

$$k_i=\lambda_i^{\mathrm{T}}\cdot z_i\cdot\lambda_i$$

The assembly of the local stiffness matrices in the global stiffness matrix is made according to the criteria illustrated in Huebner et al. (2001).

At the end of this stage, the matrix of the global stiffness K constituted by $(3n+3)\times(3n+3)$ elements, where n is the total number of nodes, and the vectors of the unknown displacements q and the nodal forces F, both of them constituted by $(3n+3)$ elements, is obtained.

$$K\cdot q=F\tag{7}$$

$$\begin{pmatrix}k_{1,a} & k_{1,b} & 0 & 0 & 0 & 0\\ k_{1,c} & (k_{1,d}+k_{2,a}) & k_{2,b} & 0 & 0 & 0\\ 0 & k_{2,c} & (k_{2,d}+k_{3,a}) & k_{3,b} & 0 & 0\\ 0 & 0 & k_{3,c} & (k_{3,d}+k_{4,a}) & \cdots & 0\\ 0 & 0 & 0 & \cdots & \cdots & k_{n,b}\\ 0 & 0 & 0 & 0 & k_{n,c} & k_{n,d}\end{pmatrix}\cdot\begin{pmatrix}q_1\\q_2\\q_3\\\cdots\\\cdots\\q_{n+1}\end{pmatrix}=\begin{pmatrix}F_1\\F_2\\F_3\\\cdots\\\cdots\\F_{n+1}\end{pmatrix}\tag{8}$$

where $k_{i,a}$, $k_{i,b}$, $k_{i,c}$, $k_{i,d}$ is the sub-matrices of k, each of them of 3×3 dimension:

$$k_i=\begin{pmatrix}k_{i,a} & k_{i,b}\\ k_{i,c} & k_{i,d}\end{pmatrix}$$

q_1, q_2, $q_3,\ldots,q_{n+1}$ are the sub-vectors composed of the three displacements of each node; F_1, F_2, $F_3,\ldots,F_{n+1}$ are the sub-vectors composed of the three external forces applied to each node.

Some of the elements of the stiffness matrix K are modified along the diagonal to consider the presence of the interaction springs connected to the nodes of the structure.

$$K^*_{3i-2,3i-2}=K_{3i-2,3i-2}+k_{t,i}\cdot\cos^2\left(\frac{\alpha_{i+1}}{2}+\frac{\alpha_i}{2}-\frac{\pi}{2}\right)\tag{9}$$

$$K^*_{3i-1,3i-1}=K_{3i-1,3i-1}+k_{t,i}\cdot\sin^2\left(\frac{\alpha_{i+1}}{2}+\frac{\alpha_i}{2}-\frac{\pi}{2}\right)\tag{10}$$

$$K^*_{3i-1,3i-2}=K_{3i-1,3i-2}+k_{t,i}\cdot\sin\left(\frac{\alpha_{i+1}}{2}+\frac{\alpha_i}{2}-\frac{\pi}{2}\right)\cdot\cos\left(\frac{\alpha_{i+1}}{2}+\frac{\alpha_i}{2}-\frac{\pi}{2}\right)\tag{11}$$

$$K^*_{3i-2,3i-1}=K_{3i-2,3i-1}+k_{t,i}\cdot\sin\left(\frac{\alpha_{i+1}}{2}+\frac{\alpha_i}{2}-\frac{\pi}{2}\right)\cdot\cos\left(\frac{\alpha_{i+1}}{2}+\frac{\alpha_i}{2}-\frac{\pi}{2}\right)\tag{12}$$

where i is the number of the generic node; $k_{t,i}$ is the normal stiffness of the interaction spring connected to node i; α_i and α_{i+1} are the angle between the local and global reference systems, for the element i and for the element $i+1$.

The constraints of the structure are placed by simply eliminating, from the stiffness matrix, the rows and columns that refer to the nodal displacement that is prevented by the constraint. The dimension of K therefore reduces in function of the number of degrees of freedom that have been eliminated by the constraints.

The vector of the nodal displacements q having been obtained from Eq. (7), it is then possible to evaluate the stress characteristics at the nodes of the structure. In practice, a conversion of the nodal displacements $q_{h\div j,i}$ is performed at the local reference system of the generic element i and, once the vector s_i is calculated, the characteristics of stress C_i at the nodes can be determined immediately through the local stiffness matrix:

$$s_i=\lambda_i\cdot q_{h\div j,i}\tag{13}$$

$$C_i=z_i\cdot s_i\tag{14}$$

3. The rock–support interaction

The rock mass interacts with the support in two ways: through the normal springs connected to the nodes of the structure (Fig. 3) and through applied active loads (q_{v} and q_{h} in Fig. 1). The normal springs allow the reaction produced by the rock to be simulated when the support, which deforms under the applied active loads, moves towards the rock.

The reaction of the rock can be described through the pressure–displacement relation (p–δ), which, in the FEM-SUP calculation code, has been considered as being of a non-linear (hyperbolic) type (Fig. 4):

$$p=p_{\mathrm{lim}}\cdot\left(1-\frac{p_{\mathrm{lim}}}{p_{\mathrm{lim}}+\eta_0\cdot\delta}\right)\tag{15}$$

where p_{lim} is maximum reaction pressure that the rock mass can offer; η_0 is the initial stiffness (for values of δ close to 0) of the rock mass.

This relation represents the simplest way to describe, without any artificial edge, the behaviour of the rock mass, when the initial stiffness and the limit pressure are known with a certain confidence. From the plate loading test in the rock masses it is possible to note a curve load–displacement that is very similar to the hyperbolic one (AFTES guidelines on the plate loading test of the rock mass).

The apparent stiffness η^* of the rock is given by the ratio p/δ that can be obtained at each node of the support structure, that is, from:

$$\eta^* = \frac{p_{lim}}{\delta} \cdot \left(1 - \frac{p_{lim}}{p_{lim} + \eta_0 \cdot \delta}\right) \tag{16}$$

The evaluation of the initial rock stiffness η_0 (bedding stiffness) requires a "volume of influence" (v.o.i.) to be identified in the rock mass for each spring (Oreste, 1999). The v.o.i. has the shape of a parallelepipedon with a width that is equal to the distance between the springs $((L_i + L_{i+1})/2)$, a thickness equal to the unitary study depth (along the tunnel axis) (1 m) and a height equal to the depth of influence (λ) inside the rock mass. λ is the distance from the tunnel perimeter at which the tensional effects produced by the action of the support have ceased to exist: therefore, it can be assumed that, at a distance of λ in the rock mass, the displacements induced by the action of the support structure are nil and that a fixed point can be foreseen for the normal springs at this location.

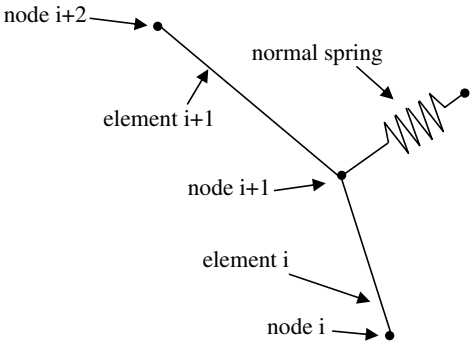

Fig. 3. Details of the rock–support interaction through Winkler springs connected to the support nodes.

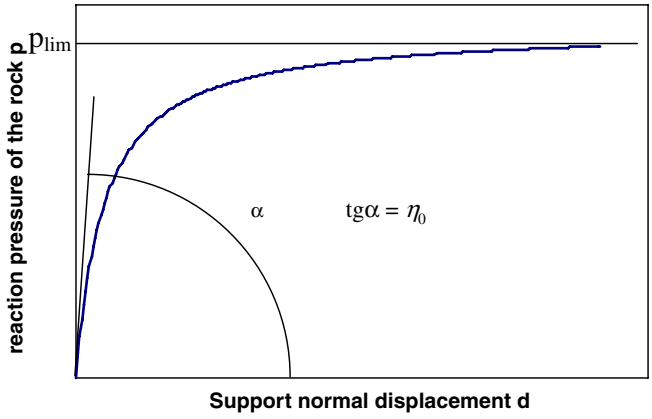

Fig. 4. Non-linear relation between the reaction pressure of the rock and the displacement of the support (p–δ). The value of the initial stiffness of the rock mass is equal to η_0 and the maximum pressure p_{lim} is reached for very high values of δ. α is equal to $\arctan(\eta_0)$.

The stiffness η_0 can be estimated using the following simplified expression (United States Army Corps of Engineers, 1997):

$$\eta_0 \cong 1.5 \cdot \frac{E_0}{D_{eq}} \tag{17}$$

E_0 is the initial elastic modulus of the rock mass; D_{eq}: the equivalent diameter of the tunnel.

The value of the maximum reaction pressure p_{lim} can be preliminary and prudently estimated starting from the cohesion values c_{rm} and the friction angle φ_{rm} of the rock mass, under the hypothesis of zero confining pressure:

$$p_{lim} = \frac{2 \cdot c_{rm} \cdot \cos\varphi_{rm}}{1 - \sin\varphi_{rm}} \tag{18}$$

When the tunnel overburden is great, the tangential stresses on the tunnel perimeter (confining pressure) cannot be negligible and so to the limit pressure of Eq. (18) this second term has to be added: $(1 + \sin\varphi_{rm})/(1 - \sin\varphi_{rm}) \cdot \Delta\sigma_{con}$, where $\Delta\sigma_{con}$ is the confining pressure on the tunnel perimeter.

The stiffness $k_{t,i}$ of each spring is simply given by the product of η_i^* (evaluated in the node to which the spring is connected to) for the area of competence of that node:

$$\begin{aligned} k_{t,i} &= \eta_i^* \cdot \left[\frac{(L_{i-1} + L_i)}{2} \cdot 1\right] \\ &= \frac{p_{lim}}{\delta_i} \cdot \left(1 - \frac{p_{lim}}{p_{lim} + \eta_0 \cdot \delta_i}\right) \cdot \frac{(L_{i-1} + L_i)}{2} \end{aligned} \tag{19}$$

As δ_i are functions of the nodal displacements q_i, the unknowns of the problem, it results that also the stiffnesses $k_{t,i}$ of the springs connected to the nodes of the structure are functions of the unknown nodal displacements. The solution is reached through successive iterations, initially placing $\eta_i^* = \eta_0$ and reducing the value of η_i^* and therefore also of $k_{t,i}$ until the values of the nodal displacements obtained from the calculation are compatible with the hypothesised stiffnesses, less an error that can be considered negligible. As the displacements of the structure towards the rock vary from node to node, the stiffnesses will also be different for the hypothesised springs.

The springs disappear in zones where the support structure moves towards the tunnel: this is generally the case of the roof, but when the horizontal active loads are greater than the vertical ones, it occurs at the sidewalls. Therefore,

only compressive loads are possible in the normal direction, where the tunnel support moves towards the rock mass: springs only work in compression.

The shear stiffness at the interface rock–support was not considered: it is in fact not guaranteed that the interface can absorb shear stresses and it is very difficult to estimate the shear stiffness value. Using a numerical model was possible to note that when the shear stiffness on the interface is neglected, the bending moments are greater both in the crown and in the sidewalls. This assumed simplified hypothesis is then precautionary.

The active vertical load q_v can be estimated using very interesting direct correlations found by various authors (Barton et al., 1974; Barton, 2002; Unal, 1983; Goel et al., 1995, 1996; Singh et al., 1992, 1997; Whickam et al., 1972; Bieniawski, 1989) between the rock mass quality index and the vertical loads on the roof of the tunnel supports. In Fig. 5 are shown the graphic suggested by Barton et al. (1974) and the nomogram of Goel et al. (1995) to evaluate the vertical loads on the support structures. This method of evaluating the vertical loads are based on the monitoring of several case histories.

The horizontal loads q_h that are applied to the side walls are usually considered to be some percentage of the vertical ones. Generally, the ratio between the horizontal and vertical loads on the support structure is lower than the in situ stress ratio K_0 for a high quality rock mass, while it can be higher than K_0 for very crushed rock masses and for squeezing and swelling ground. For the Terzaghi's Rock Load Classification, as modified by Deere et al. (1970), the horizontal loads (side pressure) on the support structure are low when the geomechanical quality of the rock mass is medium or good and can become considerable when the quality of the rock mass is very poor (completely crushed rock). By analysing the potential instability of the rock mass on the tunnel sides and hypothesing a planar sliding surface, it is possible to evaluate the q_h/q_v ratio in function of the vertical load q_v, the tunnel height H, the specific weight γ and the strength parameters c_{rm} and φ_{rm} of the rock mass:

$$\frac{q_h}{q_v} = \left(1 + \frac{\gamma \cdot H}{2 \cdot q_v}\right) \cdot \left(\frac{1 - \frac{\tan \varphi_{rm}}{\tan \alpha}}{1 + \tan \varphi_{rm} \cdot \tan \alpha}\right) - \frac{c}{q_v} \cdot \left[\frac{1}{\sin \alpha \cdot (\cos \alpha + \sin \alpha \cdot \tan \varphi_{rm})}\right]$$

where α is the inclination of the sliding surface: $\alpha = \frac{\pi}{4} + \frac{\varphi_{rm}}{2}$.

4. The equivalent support concept

Apart from the interaction with the rock mass, the behaviour of the support is also influenced by its bending and normal stiffness and the restraining conditions that are assumed. The bending and normal stiffnesses depend on the elastic modulus of the support material and on the geometry of its section. The type of constraint at the foot can influence the support behaviour to a great extent and depends on the type of foundations and on the geometry of the support.

The most commonly used type of preliminary support structure in tunnels is that of steel sets inserted in a shotcrete lining. This is a composite system for which it is necessary to define a normal and a bending equivalent stiffness in order to be able to use a bi-dimensional calculation method. For this purpose, it is considered that the equivalent support is made up of a homogeneous lining of a thickness $\bar{s}$, along the entire axis of the tunnel, with an elastic modulus $\overline{E}$. If the

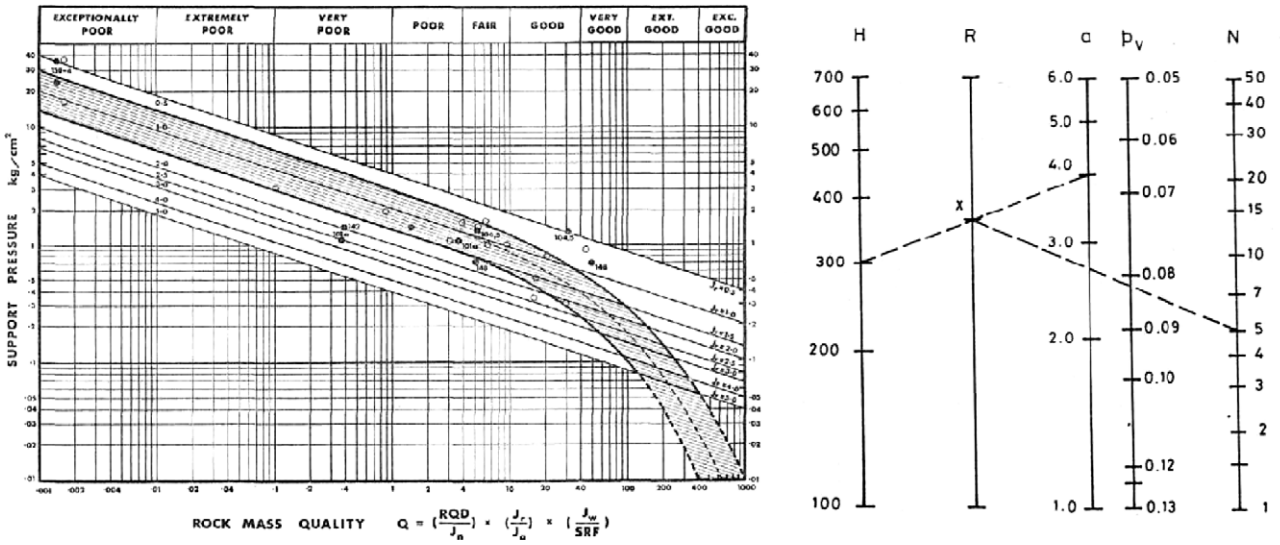

Fig. 5. On the left: Barton et al. (1974) graphic for the evaluation of vertical loads on the support structures, when Q index and J_r parameter are known. On the right: nomogram of Goel et al. (1995) for the estimation of vertical loads when the tunnel overburden H and radius a, with N index of the rock mass are known.

stiffnesses of the real system are made equal to those of the equivalent support, the following is obtained:

$$\text{normal stiffness}: \overline{E}\cdot\bar{s} = E_{\text{shot}}\cdot s_{\text{shot}} + \left(\frac{E_{\text{steel}}}{E_{\text{shot}}} - 1\right)\cdot E_{\text{shot}}\cdot\frac{A_{\text{set}}}{d} \tag{20}$$

$$\text{bendings tiffness}: \left(\overline{E}\cdot\frac{\bar{s}^3}{12}\right) = E_{\text{shot}}\cdot\frac{s_{\text{shot}}^3}{12} + \left(\frac{E_{\text{steel}}}{E_{\text{shot}}} - 1\right)\cdot E_{\text{shot}}\cdot\frac{J_{\text{set}}}{d} \tag{21}$$

where E_{shot} and E_{steel} are the elastic modulus of the shotcrete and of the steel; s_{shot} is the thickness of the shotcrete lining; A_{set} and J_{set} are the area and the moment of inertia of the section of individual steel sets; d is the spacing between the steel sets.

By resolving the system made up of Eqs. (20) and (21), it is possible to obtain:

$$\bar{s} = \sqrt{\frac{\left[E_{\text{shot}}\cdot s_{\text{shot}}^3 + 12\cdot\left(\frac{E_{\text{steel}}}{E_{\text{shot}}} - 1\right)\cdot E_{\text{shot}}\cdot\frac{J_{\text{set}}}{d}\right]}{\left[E_{\text{shot}}\cdot s_{\text{shot}} + \left(\frac{E_{\text{steel}}}{E_{\text{shot}}} - 1\right)\cdot E_{\text{shot}}\cdot\frac{A_{\text{set}}}{d}\right]}} \tag{22}$$

$$\overline{E} = \frac{\left[E_{\text{shot}}\cdot s_{\text{shot}} + \left(\frac{E_{\text{steel}}}{E_{\text{shot}}} - 1\right)\cdot E_{\text{shot}}\cdot\frac{A_{\text{set}}}{d}\right]^{\frac{3}{2}}}{\sqrt{\left[E_{\text{shot}}\cdot s_{\text{shot}}^3 + 12\cdot\left(\frac{E_{\text{steel}}}{E_{\text{shot}}} - 1\right)\cdot E_{\text{shot}}\cdot\frac{J_{\text{set}}}{d}\right]}} \tag{23}$$

It can be seen, for the usual type of supports adopted, how the thickness of the equivalent support is very similar to the thickness of the shotcrete lining ($\bar{s}\cong s_{\text{shot}}$). The stiffness of the support system can therefore be represented only by the value of the elastic modulus of the equivalent support ($\overline{E}$).

For plane strain conditions, when the support structure is continuous along the tunnel axis (i.e. shotcrete lining associated to steel sets), the elastic modulus of the equivalent support must be corrected in this following way:

$$\overline{E}^* = \frac{\overline{E}}{(1-\nu^2)}$$

5. The FEMSUP calculation code and the dimensioning of the supports

The FEMSUP calculation code, whose description is given in Appendix A in detail, is able to consider four different support geometries (Fig. 6) and five different types of constraint at the base of the steel set (Fig. 7) in an automatic way. For the sake of simplicity, only half of the tunnel is considered, because of the symmetry of the problem. The sign convention adopted by the numerical model is shown in Fig. 8.

Because of the variety of geometric forms and constraints that the calculation code is able to consider, it is suitable for the dimensioning of both preliminary supports and concrete final linings.

For geometries no. 3 and no. 4, it is possible to foresee mechanical characteristics of the support that are different in the invert arch from the remaining zones on the perimeter of the tunnel.

The programme is also able to consider:

- horizontal loads that are different from the vertical ones ($q_{\text{h}} \neq q_{\text{v}}$);
- scale parameters, that are able to deform the support along the direction x and y (m_x, m_y); the m coefficients, multiplied by the initial coordinates of the nodes, are able to modify their position and therefore the shape of the support;
- the mechanical parameters of the rock mass that condition its reaction to the deformations of the support ($c_{\text{rm}}, \varphi_{\text{rm}}, E_{\text{rm}}$).

Having defined the geometrical and mechanical parameters that influence the problem, it is possible to obtain the bending moments M, the normal force N and the shear force T along the support profile, from the calculation. These parameters and the geometry of the section of the support being known, the stresses induced inside the support structures can finally be determined.

To do this, it is usually preferred to hypothesise that the bending moments and the shear forces in the preliminary supports are entirely absorbed by the steel sets, while, as far as the normal force N is concerned, it is divided between the steel sets and the shotcrete lining on the basis of the normal stiffnesses:

$$M_{\text{set}} = M\cdot d \tag{24}$$

$$T_{\text{set}} = T\cdot d \tag{25}$$

$$N_{\text{set}} = \frac{E_{\text{steel}}\cdot A_{\text{set}}/d}{\overline{E}\cdot\bar{s}}\cdot N\cdot d = \frac{E_{\text{steel}}}{\overline{E}}\cdot\frac{A_{\text{set}}}{\bar{s}}\cdot N \tag{26}$$

$$N_{\text{shot}} = N - \frac{N_{\text{set}}}{d} \tag{27}$$

where N, M and T are the normal force, bending moment and shear force in the equivalent support per metre of tunnel, obtained using the FENSUP calculation code; N_{set}, M_{set} and T_{set} are the normal force, bending moment and shear force in each single steel set; N_{shot} is the normal force in the shotcrete per metre of tunnel.

The maximum stresses acting on the steel set ($\sigma_{\text{max,steel}}$) and in the shotcrete lining ($\sigma_{\text{max,shot}}$) are calculated using normal science of the construction techniques:

in the maximum moment point ($T_{\text{set}} = 0$):

$$\sigma_{\text{max,steel}} = \frac{M_{\text{set}}}{J_{\text{set}}}\cdot\frac{h_{\text{set}}}{2} + \frac{N_{\text{set}}}{A_{\text{set}}} \quad \sigma_{\text{max,shot}} = \frac{N_{\text{shot}}}{s_{\text{shot}}} \tag{28}$$

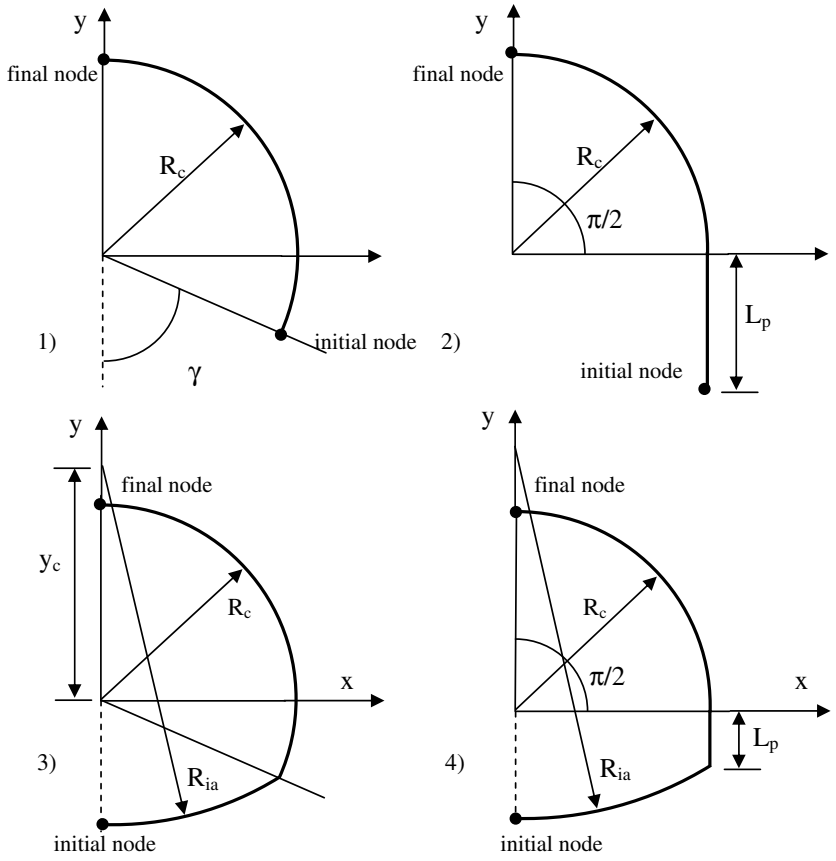

Fig. 6. Four support geometries considered in the FEMSUP calculation code. The geometric parameters required for a univocal definition of the geometry of the support structures are indicated in the figure. Key: R_{ia}: the radius of the invert arch; R_c: the crown radius; L_p: the sidewall length.

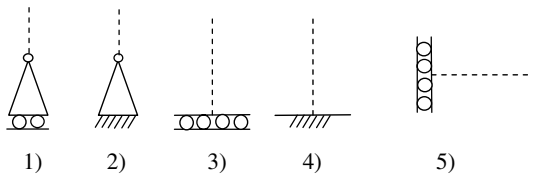

Fig. 7. Type of constraint foreseen: 1–4 for the initial node of geometries no. 1 and no. 2; 5 for the initial node of geometries no. 3 and no. 4 and for the final node of all 4 geometries. Key: (1) horizontal hinged-roller; (2) fixed hinge; (3) horizontal clamped-roller; (4) clamped; (5) vertical clamped-roller.

in the maximum normal force point ($T_{set} \neq 0$):

$$\sigma_{max,steel} = \max\left[\left(\frac{M_{set}}{J_{set}} \cdot \frac{h_{set}}{2} + \frac{N_{set}}{A_{set}}\right); \sqrt{\left(\frac{N_{set}}{A_{set}}\right)^2 + \left(\frac{3 \cdot T_{set} \cdot S_{set}}{b_{set} \cdot J_{set}}\right)^2}\right]$$

$$\sigma_{max,shot} = \frac{N_{shot}}{s_{shot}} \tag{29}$$

where h_{set} is the height of the steel set section; b_{set} is the width of the central zone of the steel set section; S_{set} is the static moment of the half-section of the steel set with respects to the barycentre axis.

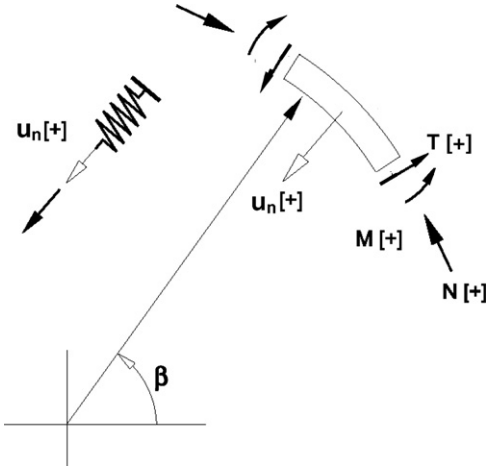

Fig. 8. Sign convention adopted by the numerical model.

The dimensioning of the support structure must be carried out in such a way that the maximum stresses induced on its inside are lower than the maximum admissible values for the materials that have been used.

An analysis for the verification of a preliminary support, made up of steel sets and shotcrete lining, performed using the FEMSUP calculation code, is here given as an example. The case refers to a road tunnel (width 14 and height 11 m),

which is at present under construction in Piedmont (North Italy). The ground involved in the excavation has poor mechanical characteristics and the maximum depth of the tunnel is 110 m. The geometrical parameters of the tunnel (scheme no. 3 of Fig. 6) are shown in Table 1, the geotechnical parameters of the ground are shown in Table 2 and the mechanical and geometric characteristics of the adopted support structure are shown in Table 3. The estimated vertical loads are 0.035 MPa, while the horizontal ones are 0.0175 MPa. The results that were obtained from the calculation are given in Table 4 and Fig. 9.

Table 1
Geometric parameters of the examined tunnel

Crown radius R_c (m)	6.15
Invert arch radius R_{ia} (m)	10.82
Height of the invert arch center y_c (m)	6.15
Scale parameter in the x direction m_x	1.14
Scale parameter in the x direction m_y	1.00

Table 2
Geotechnical parameters of the ground

Cohesion c_{rm} (MPa)	0.25
Friction angle φ_{rm}	34
Elastic modulus E_{rm} (MPa)	350

Table 3
Mechanical and geometric characteristics of the support system

Geometry of the steel set section	
Moment of inertia J_{set} (m^4)	4.276×10^{-5}
Section area A_{set} (m^2)	6.68×10^{-3}
Section height h_{set} (m)	0.20
Geometry of the support system	
Steel set spacing d (m)	1.00
Thickness of shotcrete lining s_{shot} (m)	0.22
Mechanical characteristic	
Steel elastic modulus E_{steel} (MPa)	210,000
Shotcrete elastic modulus E_{shot} (MPa)	12,000
Equivalent support characteristic	
Elastic modulus $\overline{E}$ (MPa)	16,470
Thickness $\bar{s}$ (m)	0.24

A value of the maximum stress of 75 MPa in the steel set and of 0.90 MPa in the shotcrete lining can be found from an examination of Table 4, these being values that are much lower than the maximum admissible ones. The maximum stress in the steel set can be found at the centre of the crown, while the maximum stress in the shotcrete lining is obtained in correspondence to the invert arch.

From the graph of Fig. 9 it is possible to note how the maximum moment is located at the centre of the crown and a consistent relative maximum is present in correspondence to the back. Other relative maximums of the moment, but of lower entity, can be found on the sidewalls and in the invert arch. The normal forces N are almost constant in the invert arch and in the sidewalls, but tend to diminish on the back and in the crown: they reach a minimum at the centre of the crown. The shear forces show a peak in correspondence to the invert arch-sidewall connection and a maximum relative between the back and the centre of the crown. The reaction pressure supplied by the ground following the displacements of the support is very high in correspondence to the base of the sidewall, while it is obviously nil in the area of the crown where the structure tends to move towards the centre of the tunnel.

6. Validation of the proposed numerical model

In order to validate the proposed approach a simplified example (Fig. 10) was studied also using the commonly employed numerical method FLAC (Itasca Consulting Group, 1994) which uses a difference finite approach. The comparison with analytical methods resulted to be difficult because FEMSUP applies external active loads and reaction loads on the nodes of the FEM model, while closed form solutions consider external loads as distributed pressures. FLAC code allows to compile routines with the language FISH; a specific fish program, which permits to consider the same interaction principles of the FEMSUP code (Fig. 3), was realized. The support structure was made up of 40 elements and four different cases have been considered in regard to the linkage in point A (Fig. 10): case (1):

Table 4
Calculation results

	Crown center	Back	Sidewall	Invert
Equivalent support				
Bending moment M (MN × m/m)	0.0272	−0.0227	0.0081	0.0135
Normal force N (MN/m)	0.2122	0.2695	0.2991	0.3075
Shear force T (MN/m)	0	0	0	0
Steel set				
Steel set bending moment M_{set} (MN/m)	0.0272	−0.0227	0.0081	0.0135
Steel set normal force N_{set} (MN)	0.0751	0.0954	0.1059	0.1089
Maximum stress in the steel set $\sigma_{set,max}$ (MPa)	75	67	35	48
Shotcrete lining				
Normal force in the shotcrete lining N_{shot} (MN)	0.1371	0.1741	0.1932	0.1986
Maximum stress in shotcrete $\sigma_{shot,max}$ (MPa)	0.62	0.79	0.88	0.90

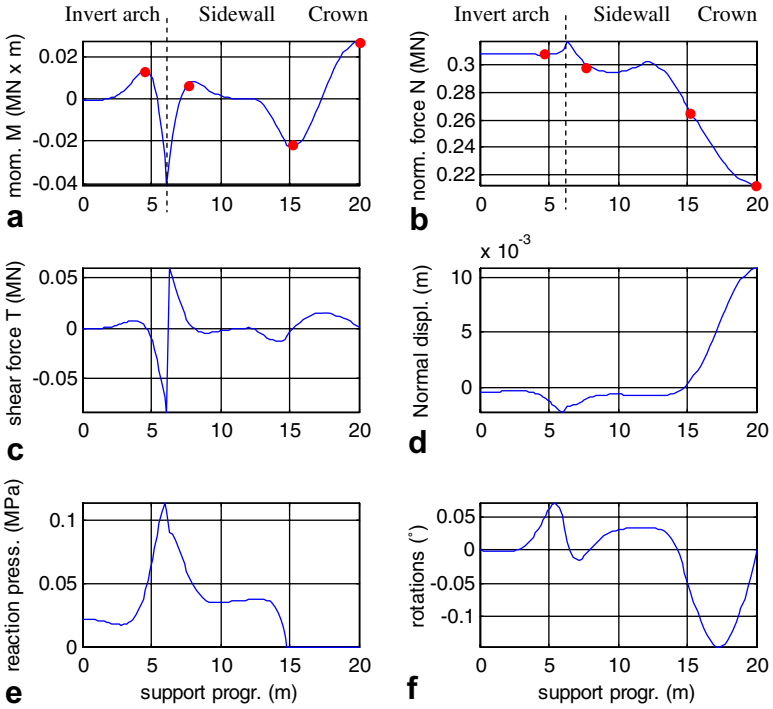

Fig. 9. Results obtained from the calculation for the equivalent support. Key: (a) bending moments along the support; (b) normal force; (c) shear force; (d) normal displacements (positive towards the inside of the tunnel); (e) reaction pressure of the ground; (f) rotation of the support structure. The points along the support in which the internal stresses in the steel sets and in the shotcrete lining were obtained are shown with circles.

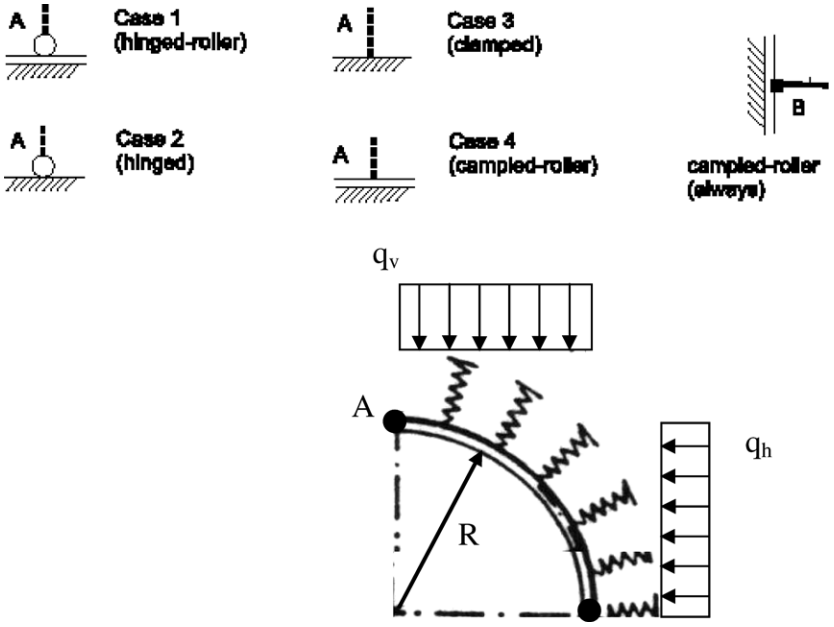

Fig. 10. Simplified calculation example used for the validation of the proposed approach with a commonly used numerical method (FLAC): $q_v = 3.33$ MPa, $q_h = 1.87$ MPa, $\eta_0 = 200$ GPa/m, $\bar{E} = 30$ GPa, $\bar{s} = 0.4$ m, $R = 4$ m.

horizontal hinged-roller constraint; case (2): hinged; case (3): clamped; case (4): horizontal clamped-roller. A vertical clamped-roller constraint was assumed in point *B*. A horizontal load equal to half of the vertical load was applied to the support.

Always the same results were obtained by FLAC and FEMSUP code for all the four studied cases. In Fig. 11 are shown some of these results for the case 2 (simple hinged constraint assumed in point *A*). This type of constraint forces nil normal displacements and bending

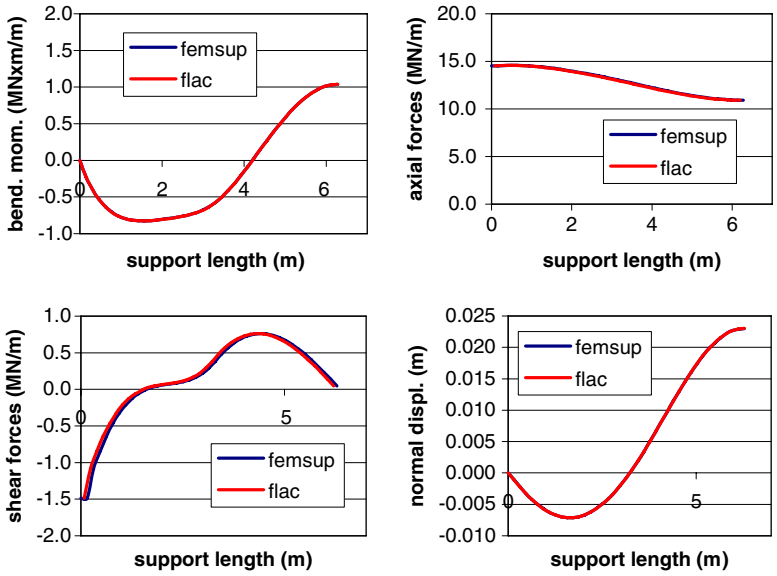

Fig. 11. Comparison results (bending moments, axial force, shear force and normal displacement along the support) of the simplified example of Fig. 10 for the case 2 (linkage in point A: fixed hinge). Support length (that is the circumferential distance along the support, measured from point A) is equal to 0 for the point A and reach its maximum value for the point B.

moments in point A. While the clamped-roller constraint in point B forces only nil shear forces (and rotations).

7. Parametric analysis and design tables

Two extensive parametric analyses were developed in order to better investigate the effects of the geomechanical quality of the rock mass, the stiffness of the support structure and the applied loads on the value of the maximum moments and the axial forces in the equivalent support. The first analysis (a) was developed for the geometry of the support given as an example in the Section 5 (Table 1), while the second (b) was for a geometry that was similar to the first, but without the invert arch. The geometrical parameters of the second geometry that was studied (b) are given in Table 5 and they refer to scheme 2 of Fig. 6. The constraint that was adopted at the base of the sidewall in geometry b is that of a hinge (type of constraint no. 2 of Fig. 7). This type of constraint results the more suitable when the steel set is founded in a groove in the ground (the typical case) later filled with shotcrete. In this case the steel set foot can not move but only rotate.

Four support systems (steel set + shotcrete lining) were used in the calculation: light (L), medium (M), heavy (H) and massive (MV). The mechanical characteristics and the geometries of each of these systems are reported in Table 6.

Table 5
Support parameters for geometry b

Crown radius R_c (m)	7.00
Height of the sidewall L_p (m)	2.50
Scale parameter in the x direction m_x	1.00
Scale parameter in the y direction m_y	1.00

Four rock masses were also considered; these were characterised by their geomechanical qualities: RMR = 25, 35, 45 and 55. The geomechanical parameters of the rock mass that intervene in the support-rock interaction were obtained for each RMR value: cohesion, friction angle and elastic modulus (Table 7). The analysis relative to RMR = 55 was not performed for geometry (a) as invert arches are not usually installed for preliminary supports in rock masses with this geomechanical quality.

Vertical loads of between 0.025 and 0.25 MPa were applied to the support, for intervals of 0.025 MPa. Three different q_h/q_v ratios were analysed: 0.33, 0.66 and 1.

Tunnel dimensions equal to 50% ($\beta = 0.5$), 75% ($\beta = 0.75$), 125% ($\beta = 1.25$), 150% ($\beta = 1.5$) of the original ones, identified from the geometrical parameters in Tables 1 and 5, were also investigated for each of the two considered geometries.

The two parametric analyses that were developed (for geometries a and b in Fig. 12) calculated 1800 and 2400 different cases, respectively, using the FEMSUP code, in such a way as to be able to cover all the possible situations that could be encountered in design practice.

The values of the moments and the normal forces at the centre of the crown (1), on the back (2), in the side walls (3) and in the invert arch (4), where the maximums relative of the bending moment were obtained (Fig. 9), were identified for each of the examined cases. In these points the shear forces are obviously nil ($T = 0$).

In order to simplify the interpretation of the results, the bending moment and the normal force have been expressed as function of the load q_v and of the width of tunnel B:

$$M = \chi \cdot q_v \cdot B^2 \tag{30}$$

$$N = \mu \cdot q_v \cdot B \tag{31}$$

Table 6
Mechanical and geometrical characteristics of the four support systems adopted in the parametric study: (1) light (L); (2) medium (M); (3) heavy (H); (4) massive (MV)

	Type L	Type M	Type H	Type MV
Geometry of the steel set section				
Moment of inertia J_{set} (m^4)	9.34×10^{-6}	2.138×10^{-5}	4.276×10^{-5}	7.784×10^{-5}
Section area A_{set} (m^2)	2.28×10^{-3}	3.34×10^{-3}	6.68×10^{-3}	7.82×10^{-3}
Section height h_{set} (m)	0.16	0.20	0.20	0.24
Geometry of the support system				
Steel set spacing d (m)	1.25	1.00	1.00	1.00
Thickness of shotcrete lining s_{shot} (m)	0.20	0.22	0.22	0.25
Mechanical characteristic				
Steel elastic modulus E_{steel} (MPa)				210,000
Shotcrete elastic modulus E_{shot} (MPa)				12,000
	Type L	Type M	Type H	Type MV
Equivalent support characteristic				
Elastic modulus $\bar{E}$ (MPa)	13,600	14,200	16,470	15,900
Thickness $\bar{s}$ (m)	0.20	0.23	0.24	0.28

Table 7
Geomechanical parameters of the rock mass for the considered RMR values

	RMR = 25	RMR = 35	RMR = 45	RMR = 55
Cohesion c_{rm} (MPa)	0.23	0.33	0.46	0.66
Friction angle φ_{rm}	30	36	40	44
Elastic modulus E_{rm} (MPa)	1500	2650	4700	8350

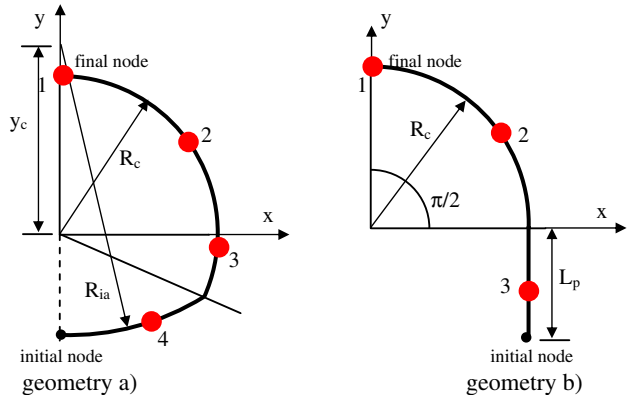

Fig. 12. Critical points in the support structure in which the values of the bending moment and the normal force were identified for each of the cases examined in the parametric analyses.

The analyses of χ and μ, with a variation of the various parameters that influence the calculation, has made it possible to draw the following conclusions:

Geometry (a) of Fig. 12:

- the value of χ in the four observation points vary quite remarkably, from 0% to 1% according to the case (in general it assumes higher values in the centre of the crown and on the back): 0.1–1% per $\beta = 0.5$, 0–0.6% per $\beta = 0.75$, 0–0.4% per $\beta \geqslant 1$;
- χ in observation points 1 and 2 tends to increase with q_v, diminish with the RMR and more slightly with k, when $\beta < 1$; it also increases with the stiffness of the support structure for $\beta < 1$; when $\beta \geqslant 1$ it is basically constant with respects to q_v, k, the RMR, the type of support used and β itself; the values of χ in observation points 1 and 2 basically result to be the same;
- χ in observation point 3 tends to increase with q_v and k, to diminish with the RMR, when $\beta \leqslant 1$; it also results to increase with the stiffness of the support structure for $\beta \leqslant 1$; when $\beta > 1$ it is basically constant with respects to q_v, k, the RMR, the type of support used and β itself;
- χ in observation point 4 tends to increase with q_v, above all for low values of the RMR, k and β; it increases with the stiffness of the support structure above all for $\beta \leqslant 1$; when $\beta > 1$ it is basically constant with respects to q_v, k, the RMR, the type of support used and β itself;
- the value of μ in the four observation points varies quite considerably, from 35% to 67%, according to the case (in general it assumes higher values on the sidewalls and in the invert arch);
- μ in observation point 1 is independent of q_v and k, while it increases slightly with a diminishing of the stiffness of the support for $\beta \leqslant 1$; it varies quite remarkably with the dimension of the tunnel for low values of β: $\mu = 35$–42% for $\beta = 0.5$, $\mu = 40$–45% for $\beta = 0.75$, $\mu = 42$–47% for $\beta \geqslant 1$;
- μ in observation point 2 is not very dependent on q_v and k, while it increases slightly with a diminishing of the stiffness of the support for $\beta \geqslant 1$; it assumes higher values than those obtained in observation point 1 ($\mu = 50$–55%);
- μ in observation point 3 is usually not very influenced by q_v, while it depends on the stiffness of the support and on k when $\beta < 1$: it diminishes with an increase in k and in the stiffness of the support; it is sensitive to the

dimensions of the tunnel: $\mu = 50$–60% for $\beta = 0.5$, $\mu = 55$–64% for $\beta = 0.75$, $\mu = 59$–65% for $\beta = 1$; $\mu = 61$–66% for $\beta = 1.25$; $\mu = 62$–67% for $\beta = 1.5$;

- μ in observation point 4 is not influenced by q_v or by k, while it depends on the stiffness of the support when $\beta < 1$: it diminishes with an increase in the stiffness of the support; it is sensitive to the dimensions of the tunnel: $\mu = 55$–61% for $\beta = 0.5$, $\mu = 60$–64% for $\beta = 0.75$, $\mu = 60$–65% for $\beta = 1$; $\mu = 60$–65% for $\beta = 1.25$; $\mu = 61$–67% for $\beta = 1.5$;

Geometry (b) of Fig. 12:

- the value of χ in the three observation points varies from 0 to 0.9% according to the case (in general it assumes higher values on the sidewalls for $k = 1$); χ is practically independent of the value of q_v;
- χ in observation point 1 tends to diminish with the RMR and increase with the stiffness of the support structure when $\beta < 1$; when $\beta \geqslant 1$ it is basically constant with respects to the RMR, the type of support used and β itself; χ results to be influenced by k, above all for $k \geqslant 0.66$;
- χ in observation point 2 tends to slightly diminish with the RMR and increase with the stiffness of the support structure when $\beta < 1$; when $\beta \geqslant 1$ it is basically constant with respects to the RMR, the type of support used and β itself; χ results to be influenced by k: it shows minimum values for $k = 0.66$ and maximum values for $k = 1$;
- χ in observation point 3 is only influenced by the value of k and β; for $k = 0.33$ and 0.66 χ is independent of β and equals 0.17 and 0.39, respectively; when $k = 1$ the following values are obtained: $\chi = 0.8$–0.92 for $\beta = 0.5$, $\chi = 0.7$–0.8 for $\beta = 0.75$, $\chi = 0.6$–0.75 for $\beta = 1$, $\chi = 0.6$–0.7 for $\beta = 1.25$ and for $\beta = 1.5$;
- the value of μ in the three observation points varies quite remarkably, from 37% to 72%, according to the case (in general it assumes higher values on the back and the sidewalls); μ is practically independent of q_v and only slightly dependent on the type of support;
- μ in observation point 1 is influenced by k for $k > 0.66$: it increases quite remarkably when passing from $k = 0.66$ to $k = 1$; for $k \leqslant 0.66$ μ equals 40I42 independently of β, while for $k = 1$ μ increases with an increase in β and passes from $\mu = 37$–38% for $\beta = 0.5$ to $\mu = 52$–58% for $\beta = 1$, and then remains practically constant for $\beta > 1$;
- μ in observation point 2 is influenced by k: it increases with an increase in k; it is equal to about 50%, independently of β for $k = 0.33$ and reaches maximum values for $k = 1$: 56–60% for $\beta = 0.5$, 60–64% for $\beta = 0.75$, 63–68% for $\beta = 1$, 64–70% for $\beta = 1.25$, 62–72% for $\beta = 1.5$;
- μ in observation point 3 is very influenced by k: it is minimum for $k = 0.66$ and reaches a maximum value for $k = 1$; it is equal to 53–58% for $k = 0.33$, it diminishes at 48–54% for $k = 0.66$ and reaches 68% for $k = 1$; with equal k it tends to increase with β.

The graphs of the calculation results (for χ and μ respectively) in the centre of the crown (critical point 1), for geometry (a) of Fig. 12 and for a ratio $q_h/q_v = 1$, are reported in Figs. 13 and 14 as an example. A certain influence of load q_v, the type of support and the geomechanical quality index RMR can be noted both for χ and for μ.

Once χ and μ are known, the type of support is chosen on the basis of a comparison of the maximum stresses in the steel and in the shotcrete, obtained from the calculation according to the criteria explained in Section 5, with the maximum admissible values for these materials.

If, for example, it is necessary to dimension the support structure of a tunnel with a shape and dimensions like those of type (a) reported in Fig. 12 ($\beta = 1$), in a rock mass which has an RMR index = 35, in which a vertical load q_v on the preliminary supports equal to 0.05 MPa and a ratio $q_h/q_v = 1$ have been estimated, the following χ and μ parameters can be obtained for the centre of the crown from Figs. 13 and 14.

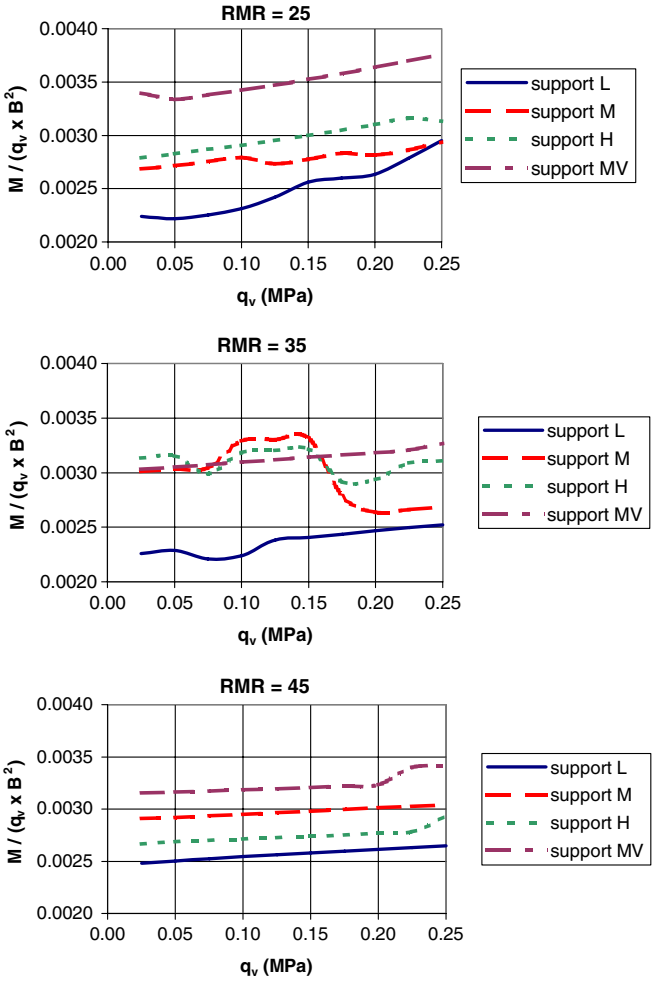

Fig. 13. Development of $\chi = M/(q_v \cdot B^2)$ with a variation of the vertical load q_v for different types of support and for an RMR = 25, 35 and 45.

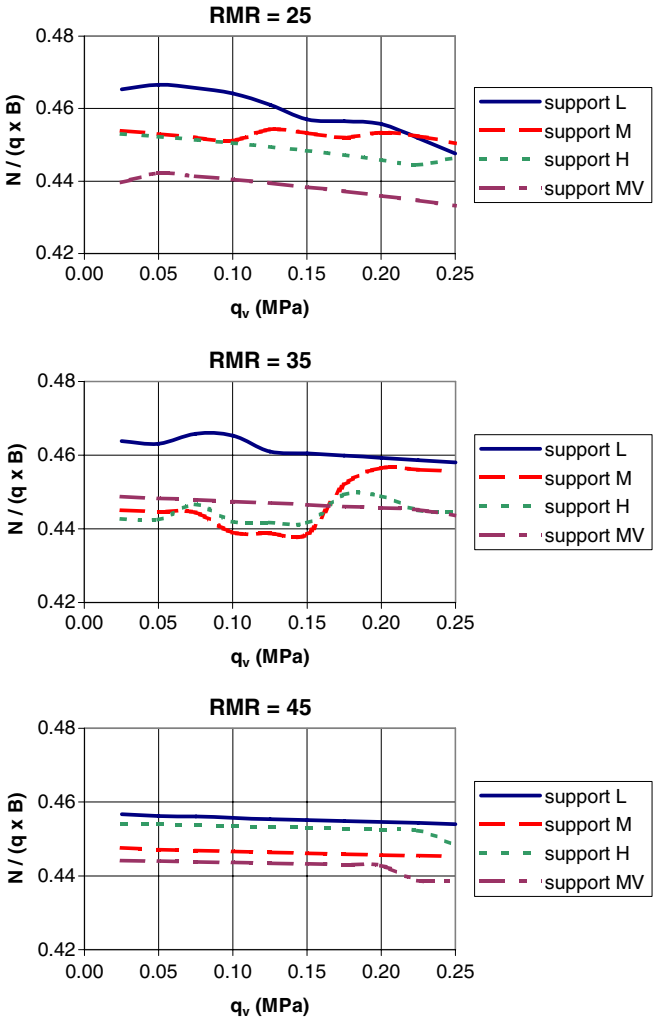

Fig. 14. Development of $\mu = N/(q_v \cdot B)$ with a variation of the vertical load q_v for different types of support and for an RMR = 25, 35 and 45.

$\chi_{1,L} = 0.00229$ $\mu_{1,L} = 0.463$
$\chi_{1,M} = 0.00303$ $\mu_{1,M} = 0.445$
$\chi_{1,H} = 0.00315$ $\mu_{1,H} = 0.442$
$\chi_{1,MV} = 0.00305$ $\mu_{1,MV} = 0.448$

In the same way, it is possible to obtain the following parameters for observation points 2 (back), 3 (sidewalls) and 4 (invert arch):

$\chi_{2,L} = 0.00208$ $\mu_{2,L} = 0.552$
$\chi_{2,M} = 0.00298$ $\mu_{2,M} = 0.544$
$\chi_{2,H} = 0.00306$ $\mu_{2,H} = 0.542$
$\chi_{2,MV} = 0.00262$ $\mu_{2,MV} = 0.547$
$\chi_{3,L} = 0.00044$ $\mu_{3,L} = 0.635$
$\chi_{3,M} = 0.00053$ $\mu_{3,M} = 0.618$
$\chi_{3,H} = 0.00059$ $\mu_{3,H} = 0.610$
$\chi_{3,MV} = 0.00067$ $\mu_{3,MV} = 0.615$
$\chi_{4,L} = 0.00117$ $\mu_{4,L} = 0.644$
$\chi_{4,M} = 0.00130$ $\mu_{4,M} = 0.628$
$\chi_{4,H} = 0.00130$ $\mu_{4,H} = 0.627$
$\chi_{4,MV} = 0.00153$ $\mu_{4,MV} = 0.632$

Once the χ and μ parameters are known, the bending moments M and the axial forces N in the equivalent support can be derived from Eqs. (30) and (31) ($q_v = 0.05$ MPa and $B = 14$ m) (Table 8).

From these values it is possible to derive the bending moment in the single steel set M_{set} ($MN \times m$), the axial forces in the single steel set N_{set} (MN) and in the shotcrete N_{shot} (MN/m), and the maximum stresses in the steel $\sigma_{max,steel}$ (MPa) and in the shotcrete $\sigma_{max,shot}$ (MPa) (Tables 9 and 10).

From an examination of the stresses in the support structure, it can be seen that, for the example under examination, the maximum values in the steel are reached in correspondence to observation points 1 (crown) and 2 (back), while the maximum values in the shotcrete are in correspondence to observation point 4 (invert arch). As a value of 220 MPa can be considered as the maximum admissible stress value in the steel, because of the provisional character of the preliminary supports, and a value of 5 MPa in the shotcrete, the adequate support for the examined case results to be of type M (medium) (Table 6).

Working in the same way for all the 4200 cases of the parametric analyses, it was possible to define indicative tables of the type of support that is necessary (Tables 11–20), with a variation of the applied load, of the coefficient k, of the geomechanical quality (RMR) and of the dimensions of the tunnel (β) for the two different geometries of the support structure. In the cases where it is not possible to identify a support type that is able to support the loads transmitted by the rock mass, it is necessary to intervene with reinforcement and consolidation works of the rock mass that lead to a reduction of the loads acting on the support structure.

The slenderness of the sidewalls was taken into account in the evaluation of the stress conditions on the sidewalls for the geometry (b). In more detail, the normal stress in the steel and in the shotcrete where the bending moment reaches a maximum value was obtained by the following Eq. (32), which substitute the Eq. (28):

$$\sigma_{max,steel} = \max\left[\frac{M_{eq}}{J_{set}\cdot\left(1-1.5\cdot\frac{N_{set}}{N_{cr}}\right)}\cdot\frac{h_{set}}{2}+\omega_{set}\cdot\frac{N_{set}}{A_{set}};\frac{M_{max}}{J_{set}}\cdot\frac{h_{set}}{2}+\omega_{set}\cdot\frac{N_{set}}{A_{set}}\right]$$

$$\sigma_{max,shot} = \omega_{shot}\cdot\frac{N_{shot}}{s_{shot}} \qquad (32)$$

where M_{eq} is equivalent bending moment in the steel set (sidewalls): $M_{eq} = 1.3 \cdot M_{med}$ with $0.75 \cdot M_{max} \leqslant M_{eq} \leqslant M_{max}$; M_{med} and M_{max} mean and maximum bending moment in the sidewall steel set; N_{cr} is Eulerian critical axial force: $N_{cr} = \frac{\pi^2 \cdot E_{st} \cdot A_{set}}{\lambda_{set}^2}$; λ_{set} is slenderness of the sidewall steel set: $\lambda_{set} = l_p/\sqrt{J_{set}/A_{set}}$; l_p: sidewall length; ω_{set} is a factor

Table 8
Bending moments and normal forces in the equivalent support, in correspondence to the 4 observation points where the bending moment shows a relative maximum

Observation points	Type of support			
	L (light)	M (medium)	H (heavy)	MV (massive)
1 (crown center)				
M (MN × m/m)	0.0224	0.0297	0.0309	0.0299
N (MN/m)	0.324	0.312	0.309	0.314
2 (back)				
M (MN × m/m)	0.0204	0.0292	0.0300	0.0257
N (MN/m)	0.386	0.381	0.379	0.383
3 (sidewalls)				
M (MN × m/m)	0.0043	0.0052	0.0058	0.0066
N (MN/m)	0.445	0.433	0.427	0.431
4 (invert arch)				
M (MN × m/m)	0.0115	0.0127	0.0127	0.0150
N (MN/m)	0.451	0.440	0.439	0.442

Table 9
Bending moments and normal forces in the steel set and in the shotcrete lining, in correspondence to the 4 observation points where the bending moment shows a relative maximum value

Observation points	Type of support			
	L (light)	M (medium)	H (heavy)	MV (massive)
1 (crown center)				
M_{set} (MN × m)	0.0281	0.0297	0.0309	0.0299
N_{set} (MN)	0.0562	0.0662	0.1095	0.1132
N_{shot} (MN/m)	0.2791	0.2453	0.1999	0.2004
2 (back)				
M_{set} (MN × m)	0.0255	0.0292	0.0300	0.0257
N_{set} (MN)	0.0670	0.0809	0.1343	0.1382
N_{shot} (MN/m)	0.3328	0.2999	0.2451	0.2447
3 (sidewalls)				
M_{set} (MN × m)	0.0054	0.0052	0.0058	0.0066
N_{set} (MN)	0.0771	0.0919	0.1512	0.1554
N_{shot} (MN/m)	0.3828	0.3407	0.2758	0.2751
4 (invert arch)				
M_{set} (MN × m)	0.0143	0.0127	0.0127	0.0150
N_{set} (MN)	0.0782	0.0934	0.1554	0.1597
N_{shot} (MN/m)	0.3883	0.3462	0.2835	0.2827

Table 10
Maximum stresses in the steel and in the shotcrete, in correspondence to the 4 observation points where the bending moment shows a relative maximum value

Observation points	Type of support			
	L (light)	M (medium)	H (heavy)	MV (massive)
1 (crown center)				
$\sigma_{max,steel}$ (MPa)	265	159	89	61
$\sigma_{max,shot}$ (MPa)	1.40	1.12	0.91	0.80
2 (back)				
$\sigma_{max,steel}$ (MPa)	248	161	90	57
$\sigma_{max,shot}$ (MPa)	1.66	1.36	1.11	0.98
3 (sidewalls)				
$\sigma_{max,steel}$ (MPa)	80	52	36	30
$\sigma_{max,shot}$ (MPa)	1.91	1.55	1.25	1.10
4 (invert arch)				
$\sigma_{max,steel}$ (MPa)	157	88	53	44
$\sigma_{max,shot}$ (MPa)	1.94	1.57	1.29	1.13

Table 11
Support typology necessary for geometry (a) of Fig. 12 and for $\beta = 0.5$ ($B = 7$ m), with a variation of q_v, k and RMR

q_v (MPa)	RMR = 25			RMR = 35			RMR = 45		
	$k = 0.33$	$k = 0.66$	$k = 1.00$	$k = 0.33$	$k = 0.66$	$k = 1.00$	$k = 0.33$	$k = 0.66$	$k = 1.00$
0.025	L	L	L	L	L	L	L	L	L
0.050	L	L	L	L	L	L	L	L	L
0.075	M	M	M	L	L	L	L	L	L
0.100	M	M	M	M	M	M	M	M	M
0.125	H	M	M	M	M	M	M	M	M
0.150	H	H	H	H	H	H	M	M	M
0.175	H	H	H	H	H	H	H	H	H
0.200	H	H	H	H	H	H	H	H	H
0.225	MV	MV	H	H	H	H	H	H	H
0.250	MV	MV	MV	MV	MV	H	H	H	H

Table 12
Support typology necessary for geometry (a) of Fig. 12 and for $\beta = 0.75$ ($B = 10.5$ m), with a variation of q_v, k and RMR

q_v (MPa)	RMR = 25			RMR = 35			RMR = 45		
	$k = 0.33$	$k = 0.66$	$k = 1.00$	$k = 0.33$	$k = 0.66$	$k = 1.00$	$k = 0.33$	$k = 0.66$	$k = 1.00$
0.025	L	L	L	L	L	L	L	L	L
0.050	L	L	L	L	L	L	L	L	L
0.075	M	M	M	M	M	M	M	M	M
0.100	H	H	M	M	M	M	M	M	M
0.125	H	H	H	H	H	H	H	H	H
0.150	H	H	H	H	H	H	H	H	H
0.175	MV	MV	MV	H	H	H	H	H	H
0.200	–	MV	MV	MV	MV	MV	MV	MV	MV
0.225	–	–	–	–	MV	MV	MV	MV	MV
0.250	–	–	–	–	–	–	–	–	–

Table 13
Support typology necessary for geometry (a) of Fig. 12 and for $\beta = 1$ ($B = 14$ m), with a variation of q_v, k and RMR

q_v (MPa)	RMR = 25			RMR = 35			RMR = 45		
	$k = 0.33$	$k = 0.66$	$k = 1.00$	$k = 0.33$	$k = 0.66$	$k = 1.00$	$k = 0.33$	$k = 0.66$	$k = 1.00$
0.025	L	L	L	L	L	L	L	L	L
0.050	M	M	M	M	M	M	M	M	M
0.075	M	M	M	M	M	H	H	H	H
0.100	H	H	H	H	H	H	H	H	H
0.125	H	H	H	H	H	H	MV	H	H
0.150	MV	MV	MV	MV	MV	MV	MV	MV	MV
0.175	–	–	–	MV	MV	MV	MV	MV	MV
0.200	–	–	–	–	–	–	–	–	–
0.225	–	–	–	–	–	–	–	–	–
0.250	–	–	–	–	–	–	–	–	–

Table 14
Support typology necessary for geometry (a) of Fig. 12 and for $\beta = 1.25$ ($B = 17.5$ m), with a variation of q_v, k and RMR

q_v (MPa)	RMR = 25			RMR = 35			RMR = 45		
	$k = 0.33$	$k = 0.66$	$k = 1.00$	$k = 0.33$	$k = 0.66$	$k = 1.00$	$k = 0.33$	$k = 0.66$	$k = 1.00$
0.025	L	L	M	L	M	L	M	L	L
0.050	M	M	H	M	M	M	H	M	M
0.075	H	H	H	H	H	H	H	H	H
0.100	H	H	H	H	H	H	MV	MV	H
0.125	MV	MV	MV	MV	MV	MV	–	–	MV
0.150	–	–	–	–	–	–	–	–	–
0.175	–	–	–	–	–	–	–	–	–
0.200	–	–	–	–	–	–	–	–	–
0.225	–	–	–	–	–	–	–	–	–
0.250	–	–	–	–	–	–	–	–	–

Table 15
Support typology necessary for geometry (a) of Fig. 12 and for $\beta = 1.5$ ($B = 21$ m), with a variation of q_v, k and RMR

q_v (MPa)	RMR = 25			RMR = 35			RMR = 45		
	$k = 0.33$	$k = 0.66$	$k = 1.00$	$k = 0.33$	$k = 0.66$	$k = 1.00$	$k = 0.33$	$k = 0.66$	$k = 1.00$
0.025	M	M	L	M	L	M	M	M	M
0.050	H	H	H	H	H	H	H	H	H
0.075	H	H	MV	MV	MV	H	MV	H	H
0.100	MV	MV	–	–	–	MV	–	MV	MV
0.125	–	–	–	–	–	–	–	–	–
0.150	–	–	–	–	–	–	–	–	–
0.175	–	–	–	–	–	–	–	–	–
0.200	–	–	–	–	–	–	–	–	–
0.225	–	–	–	–	–	–	–	–	–
0.250	–	–	–	–	–	–	–	–	–

Table 16
Support typology necessary for geometry (b) of Fig. 12 and for $\beta = 0.5$ ($B = 7$ m), with a variation of q_v, k and RMR

q_v (MPa)	RMR = 25			RMR = 35			RMR = 45			RMR = 55		
	$k = 0.33$	$k = 0.66$	$k = 1.00$	$k = 0.33$	$k = 0.66$	$k = 1.00$	$k = 0.33$	$k = 0.66$	$k = 1.00$	$k = 0.33$	$k = 0.66$	$k = 1.00$
0.025	L	L	L	L	L	L	L	L	L	L	L	L
0.050	L	L	L	L	L	L	L	L	L	L	L	L
0.075	L	L	M	L	L	M	L	L	M	L	L	M
0.100	L	L	M	L	L	M	L	L	M	L	L	M
0.125	M	M	H	L	M	H	L	M	H	L	M	H
0.150	M	M	H	M	M	H	M	M	H	M	M	H
0.175	M	M	H	M	M	H	M	M	H	M	M	H
0.200	M	M	MV	M	M	MV	M	M	MV	M	M	MV
0.225	H	H	MV	M	H	MV	M	H	MV	M	H	MV
0.250	H	H	MV	H	H	MV	H	H	MV	H	H	MV

Table 17
Support typology necessary for geometry (b) of Fig. 12 and for $\beta = 0.75$ ($B = 10.5$ m), with a variation of q_v, k and RMR

q_v (MPa)	RMR = 25			RMR = 35			RMR = 45			RMR = 55		
	$k = 0.33$	$k = 0.66$	$k = 1.00$	$k = 0.33$	$k = 0.66$	$k = 1.00$	$k = 0.33$	$k = 0.66$	$k = 1.00$	$k = 0.33$	$k = 0.66$	$k = 1.00$
0.025	L	L	L	L	L	L	L	L	L	L	L	L
0.050	L	M	M	L	M	M	L	M	M	L	M	M
0.075	L	M	H	L	M	H	L	M	H	M	M	H
0.100	M	M	H	M	M	H	M	M	H	M	M	H
0.125	M	H	MV	M	H	MV	M	H	MV	M	H	MV
0.150	M	H	–	M	H	–	M	H	–	M	H	–
0.175	H	H	–	H	H	–	H	H	–	H	H	–
0.200	H	MV	–	H	MV	–	H	MV	–	H	MV	–
0.225	H	MV	–	H	MV	–	H	MV	–	H	MV	–
0.250	H	MV	–	H	MV	–	H	MV	–	H	MV	–

Table 18
Support typology necessary for geometry (b) of Fig. 12 and for $\beta = 1$ ($B = 14$ m), with a variation of q_v, k and RMR

q_v (MPa)	RMR = 25			RMR = 35			RMR = 45			RMR = 55		
	$k = 0.33$	$k = 0.66$	$k = 1.00$	$k = 0.33$	$k = 0.66$	$k = 1.00$	$k = 0.33$	$k = 0.66$	$k = 1.00$	$k = 0.33$	$k = 0.66$	$k = 1.00$
0.025	L	L	M	L	L	M	L	L	M	L	L	M
0.050	L	M	H	L	M	H	L	M	H	M	L	H
0.075	M	H	MV	M	H	MV	M	H	MV	M	M	MV
0.100	M	H	–	M	H	–	M	H	–	H	H	–
0.125	H	MV	–	H	MV	–	H	MV	–	H	MV	–
0.150	H	MV	–	H	MV	–	H	MV	–	H	MV	–
0.175	H	–	–	H	–	–	H	–	–	MV	–	–
0.200	H	–	–	H	–	–	MV	–	–	MV	–	–
0.225	MV	–	–	MV	–	–	MV	–	–	–	–	–
0.250	MV	–	–	MV	–	–	MV	–	–	–	–	–

Table 19
Support typology necessary for geometry (b) of Fig. 12 and for $\beta = 1.25$ ($B = 17.5$ m), with a variation of q_v, k and RMR

q_v (MPa)	RMR = 25			RMR = 35			RMR = 45			RMR = 55		
	$k = 0.33$	$k = 0.66$	$k = 1.00$	$k = 0.33$	$k = 0.66$	$k = 1.00$	$k = 0.33$	$k = 0.66$	$k = 1.00$	$k = 0.33$	$k = 0.66$	$k = 1.00$
0.025	L	M	H	L	M	H	L	M	H	L	L	H
0.050	M	H	MV	M	H	MV	M	H	MV	M	L	MV
0.075	M	H	–	M	H	–	H	H	–	H	M	–
0.100	H	MV	–	H	MV	–	H	MV	–	H	H	–
0.125	H	–	–	H	–	–	H	–	–	MV	H	–
0.150	H	–	–	H	–	–	MV	–	–	MV	H	–
0.175	MV	–	–	MV	–	–	–	–	–	–	MV	–
0.200	–	–	–	–	–	–	–	–	–	–	–	–
0.225	–	–	–	–	–	–	–	–	–	–	–	–
0.250	–	–	–	–	–	–	–	–	–	–	–	–

Table 20
Support typology necessary for geometry (b) of Fig. 12 and for $\beta = 1.5$ ($B = 21$ m), with a variation of q_v, k and RMR

q_v (MPa)	RMR = 25			RMR = 35			RMR = 45			RMR = 55		
	$k = 0.33$	$k = 0.66$	$k = 1.00$	$k = 0.33$	$k = 0.66$	$k = 1.00$	$k = 0.33$	$k = 0.66$	$k = 1.00$	$k = 0.33$	$k = 0.66$	$k = 1.00$
0.025	L	M	H	L	M	H	M	L	H	L	L	H
0.050	M	H	–	M	H	–	M	M	–	M	M	–
0.075	H	MV	–	H	MV	–	H	H	–	H	M	–
0.100	H	–	–	H	–	–	H	–	–	H	H	–
0.125	MV	–	–	MV	–	–	–	–	–	–	H	–
0.150	MV	–	–	MV	–	–	–	–	–	–	MV	–
0.175	–	–	–	–	–	–	–	–	–	–	–	–
0.200	–	–	–	–	–	–	–	–	–	–	–	–
0.225	–	–	–	–	–	–	–	–	–	–	–	–
0.250	–	–	–	–	–	–	–	–	–	–	–	–

that is function of the type of the steel set section and of the sidewall steel set slenderness: $\omega_{set} \cong 9 \times 10^{-5} \cdot \lambda_{set}^2 - 0.0013 \cdot \lambda_{set} + 1.0402$ when $\lambda_{set} > 20$; ω_{shot} is a factor that is function of the sidewall shotcrete slenderness: $\omega_{shot} \cong 2 \times 10^{-4} \cdot \lambda_{shot}^2 - 0.0239 \cdot \lambda_{shot} + 1.5857$ when $\lambda_{shot} > 50$; λ_{shot} is slenderness of the sidewall shotcrete: $\lambda_{shot} = 2 \cdot \sqrt{3} \cdot (l_p/s_{shot})$.

The previously reported design tables permit indications to be made on the type of support that is necessary, in a simple and quick way, having defined the geometry of the tunnel, the geomechanical quality of the rock mass, the vertical loads foreseen on the support and the ratio k between the horizontal and vertical loads. Using these tables, it is also possible to verify the influence of the various calculation parameters on the dimensioning of the support structure, in order to decide whether it is convenient to study the unknown parameters in more detail. They are also useful during the dimensioning analyses as they help one to start with the numerical calculations considering types of support that are close to the final ones, thus saving precious time.

From an examination of the tables it can be seen how geometry (b) in Fig. 9 is more influenced by coefficient k than geometry (a). When $k = 1$, the support structures are able to bear modest loads with geometry (b), above all for large dimensions of the tunnel. In these cases, it is necessary to install the invert arch foreseen in geometry (a) or to intervene with reinforcement and consolidation techniques of the rock mass.

8. Conclusions

The hyperstatic reaction method is particularly suitable for the dimensioning of the most widely used support structures in tunnels: steel sets incorporated in a shotcrete lining. The method allows the results of the bending moment, the shear forces and the normal force along the support profile to be obtained, in reduced calculation times.

A numerical type approach to the hyperstatic reaction method has been presented in this paper and the adopted mathematical procedure, the parameters that condition the calculation and the techniques used to dimension the support structures, on the basis of the results of the method, are also given. The FEMSUP code is described. This code is able to consider the actual geometry of the support and the horizontal active loads that are different from the vertical ones; it is therefore able to analyse the rock mass-structure interaction in detail.

An extensive parametric analysis has made it possible to define the necessary support structures in a wide number of cases that cover the conditions that are generally encountered in excavation practice: four different geomechanical

quality values (described through the RMR index), ten vertical load values, three coefficient k values, two support structure geometries (with and without the invert arch), five different tunnel dimensions (from a width of 7 m to a width of 21 m) and four support types, characterised by the thickness of the shotcrete lining and by the foreseen type of steel set, were all considered. The moment and the normal force were evaluated for each case in different critical points of the support (the centre of the crown, the back, the sidewalls and the invert arch), where a maximum in the development of the bending 1moment can be observed. The maximum stresses in the steel and in the shotcrete were then calculated and compared with the maximum admissible stresses of the two materials. Finally, the most suitable type of support was chosen, on the basis of these comparisons, for each studied case.

Ten design tables were drawn up to summarise the results of the parametric analyses.

From an examination of the tables, it is possible to verify the influence of the various calculation parameters on the dimensioning of the support structure in order to be able to decide whether it is convenient to perform an in depth study of the parameters that are not precisely known. These tables are also useful during the dimensioning analyses as they allow one to start with the numerical verifications from configurations that are similar to the final calculation ones, thus saving precious time. They can also be adapted to supply rough indications on the entity of the support structures in the preliminary stages of the project or to suggest variations, during the tunnel construction, of the characteristics of the supports foreseen in the design phase, on the basis of the actually encountered rock mass geomechanical quality.

In order to carry out the calculation with the FEMSUP code or to use the design tables presented in this paper, it is necessary to know the entity of the loads applied to the support structure. In particular, it is necessary to know the vertical load q_v and the coefficient k, the ratio between the applied horizontal and vertical loads (q_h/q_v). These two important parameters can be evaluated initially on the basis of empirical relations and geomechanical indexes of the rock mass. Different empirical correlations are available in literature that are able to supply indications on q_v in function of the geomechanical quality index (RMR or Q) or of the geomechanical parameters of the rock mass. Vertical and horizontal loads can also be obtained backwards from the convergence measurements during the construction of tunnels. In this case, FEMSUP code can be useful to verify static conditions of the supports which have been defined in the design phase. There is, however, a lack of a rational organisation of knowledge in this field; this lack of knowledge on the vertical loads acting on the support structures requires further in depth scientific studies so as to be able to estimate their value, with a certain precision, under the various conditions that can be encountered during the excavation of a tunnel.

Appendix A. Detailed description of the FEMSUP calculation code

The FEMSUP calculation code has been written in MATLAB programming language and it foresees the following calculation stages:

- Definition of the elements that make up the structure;
- Automatic determination of the nodes on which the applied external loads act;
- Construction of the global stiffness matrix, starting from the local stiffness matrix;
- Modification of the global stiffness matrix in order to take the constraint conditions into consideration;
- Definition of the nodal forces in the zone in which the applied external loads act;
- Iterative calculation that foresees a progressive reduction (up to the annulment) of the stiffness of the springs which work under traction (because of the displacement of the support towards the tunnel) and the continuous modification of the stiffness of the springs which work under compression (because of the displacement of the support towards the rock), in function of the displacement value reached in the previous calculation step;
- Resolution of the system of linear equations and obtaining the nodal displacement vectors, for each step of the iterative calculation;
- Once the iterative process has finished, the nodal displacements under the global coordinates system are first converted considering the local coordinates system of each element and then multiplied by the local stiffness matrix (expressed under the local coordinates system) to obtain the nodal forces and therefore the stress states of each element;
- Plotting of the results.

The data of the problem that are necessary for the calculation are directly inserted into the programme, attributing the respective value to each variable: the name of the variable in the calculation programme is here given together with each datum:

- Type of support geometry (Fig. 6) (“geom”): this can be equal to 1, 2, 3 or 4;
- Number of elements in the support structure (for half of the tunnel) (“num_el”);
- Crown radius (“Rcal”);
- Stretching coefficient of the structure in the horizontal direction (x) (“mx”): this coefficient is multiplied by the coordinate x of each node of the structure in order to obtain a modification of the support geometry (for values of “mx” above 1, a widening of the structure is obtained, while for values below 1, a diminishing is obtained);
- Stretching coefficient of the structure in the vertical direction (y) (“my”): as for “mx”, a deformation of the structure occurs, but now in the vertical direction;

- Elastic modulus of the equivalent support in the crown and sidewall zones (“Esost1”);
- Area (thickness) of the equivalent support in the crown and sidewall zones (“Asost1”);
- Inertia moment of the equivalent support in the crown and sidewall zones (“Jsost1”);
- Initial angle of the crown development (only for geometry 1 in Fig. 6) (“gamma_in”);
- Type of constraint on the initial node (Fig. 7) (“vinc”): this can be equal to 1, 2, 3 or 4 (constraint type 5 is automatically imposed in the initial node of geometries no. 3 and no. 4 of Fig. 6);
- Length of the rectilinear sidewall (only for geometries no. 2 and no. 4 of Fig. 6) (“Lp”);
- Radius of the invert arch (only for geometries no. 3 and no. 4) (“Rar”);
- Distance between the centres of the crown and the invert arches (only for geometry no. 3) (“yc”);
- Elastic modulus of the equivalent support in the invert arch zone (geometries no. 3 and no. 4) (“Esost3”);
- Area (thickness) of the equivalent support in the invert arch zone (geometries no. 3 and no. 4) (“Asost3”);
- Inertia moment of the equivalent support in the invert arch zone (geometries no. 3 and no. 4) (“Jsost3”);
- Vertical pressure applied to the crown of the support structure (“pv”);
- Horizontal pressure applied to the sides of the support structure (“ph”);
- Cohesion of the rock mass (“c”);
- Friction angle of the rock mass (“fi”);
- Elastic modulus of the rock mass (“Eroccia”).

The first lines of the FEMSUP programme, dedicated to the input of the data of the problem, are given in the following

```
geom = 2;
num_el = 50;
Rcal = 7;
mx = .75;
my = .75;


Esost1 = 13600;
Asost1 = .2;
Jsost1 = Asost1^3/12;


if geom == 1
  gamma_in = 90/57.297;
  vinc = 1;
elseif geom == 2
  Lp = 2.5;
  vinc = 1;
elseif geom == 3
  Rar = 10.82;
  yc = 6.15;
  Esost3 = Esost1;
  Asost3 = Asost1;
  Jsost3 = Jsost1;
elseif geom == 4
  Rar = 10.9;
  Lp = 2.2;
  Esost3 = 16470;
  Asost3 = .24;
  Jsost3 = .24^3/12;
end


pv = .025;
ph = .666*pv;


c = .33;
fi = 36/57.297;
Eroccia = 2650;
```

The measurement units that have been used are those of the international system (SI): *m* for the lengths, MPa for the pressures and rad for the angles. A bi-dimensional type calculation (plain strain analysis) has been made and therefore a depth of the tunnel equal to 1 m has been considered.

At the time of writing, the FEMSUP calculation programme is available on the following website:
http://staff.polito.it/pierpaolo.oreste/index.htm

References

AFTES, 1997. Guidelines on the plate loading test of the rock mass, Tunnel et Ouvrages Souterrain.

Barton, N., 2002. Some new Q-value correlations to assist in site characterisation and tunnel design. International Journal of Rock Mechanics and Mining Sciences, 185–216.

Barton, N., Lien, R., Lunde, J., 1974. Engineering classification of rock masses for the design of tunnel support. Rock Mechanics (6), 183–236.

Bieniawski, Z.T., 1989. Engineering Rock Mass Classification. John Wiley, New York.

Bouvard-Lecoanet, A., Colombet, G., Esteulle, F., 1988. Ouvrages souterrains: conception, réalisation, entretien. Presses de l’école nationale des Ponts et chaussées, Paris.

Brown, E.T., Bray, J.W., Ladanyi, B., Hoek, E., 1983. Ground Response Curves for Rock Tunnels. Journal of Geotechnical Engineering (109), 15–39.

Deere, D.U., Peck, R.B., Parker, H., Monsees, J.E., Schmidt, B., 1970. Design of tunnel support systems. High Res. Rec. (339), 26–33.

Duddeck, H., Erdmann, J., 1985. On structural design models for tunnels in soft soil. Underground Space (9), 246–259.

Einstein, H.H., Schwartz, C.W., 1979. Simplified analysis for tunnel supports. Journal of the Geotechnical Engineering Division (April), 499–518.

Goel, R.K., Jethwa, J.L., Paithankar, A.G., 1995. Indian experience with Q and RMR systemTunnelling and Underground Space Technology, Vol. 10. Pergamon, pp. 97–109.

Goel, R.K., Jethwa, J.L., Dhar, B.B., 1996. Effect of tunnel size on support pressure, Technical note. International Journal of Rock Mechanics and Mining Science and Geomech. 33 (7), 749–755. Abstract.

Hoek, E., Brown, E.T., 1980. Underground Excavations in Rock. The Institution of Mining and Metallurgy, London, 527 p.

Huebner, K.H., Dewhirst, D.L., Smith, D.E., Byrom, T.G., 2001. The Finite Element Method for Engineers. John Wiley and Sons, inc., New York.

Leca, E., Clough, W., 1992. Preliminary design for NATM tunnel support in soil. Journal of Geotechnical Engineering 118 (4), 558–575.

Oreste, P., 1999. Important aspects of the analysis and dimensioning of tunnel supports through numerical methods. Gallerie e Grandi Opere Sotterranee, April 1999, 57:39–50.

Oreste, P., 2003. Analysis of Structural Interaction in Tunnels using the Convergence-Confinement Approach. Tunnelling and Underground Space Technology. Pergamon Press, Oxford.

Panet, M., 1995. Le calcul des tunnels par la méthode convergence-confinement. Presses de l'école nationale des Ponts et chaussées, Paris.

Rechsteiner, G.F., Lombardi, G., 1974. Une methode de calcul elasto-plastique de l'état de tension et de deformation autour d'une cavite souterraine. In: Advances in rock mechanics, Proceedings of the Third Congress of the International Society for Rock Mechanics, pp. 1049–1054.

Singh, B., Jethwa, J.L., Dube, A.K., Singh, B., 1992. Correlation between observed support pressure and rock mass qualityTunnelling and underground space technology, Vol. 7. Pergamon, pp. 59–75.

Singh, B., Goel, R.K., Jethwa, J.L., Dube, A.K., 1997. Support pressure assessment in arched underground openings through poor rock massesEngineering Geology, Vol. 48. Elsevier Science, 59–81.

Unal, E., 1983. Design guidelines and roof control standards for coal mine roofs, Ph.D. Thesis, Pennsylvania State University.

U.S.A.C.E. (United States Army Corps of Engineers), 1997. Tunnels and Shafts in Rocks: Engineering and Design, chapter 9. Washington D.C.